Numerical Investigation of the Vortex System on Forebody of an Aircraft at High Angles of Attack Applied to the Problem of Providing Directional Stability

Kirill Makarov and Alexander A. Pavlenko**
** Central Aero-Hydrodynamic Institute n.a. Prof. Zhukovsky*
1 Zhukosvsky str., Zhukovsky, Moscow Region, Russia, 140180

Abstract

Computational fluid dynamics has been used to study the subsonic flowfield over a chine-shaped forebody of a research aircraft model at high angles of attack and moderate sideslips. The results of simulation show the presence of a system of two vortices formed at the apex of the forebody. The asymmetry in the strength and positions of these vortices at high angles of attack and nonzero side-sleep angle results in increasing rarefication at the windward side of the forebody and decreasing it at the leeward one which in turn results in improving the directional stability of the model. Computational results have been supplemented with the wind tunnel experimental data.

1. Introduction

One of the modern requirements for maneuverable aircraft is to ensure high lifting properties, stability and controllability at high and very high angles of attack. Experimental studies and in-flight testings of aircraft show that at high angles of attack flow around forebody was accompanied by the formation of intense vortex system, which can lead to large destabilizing yaw moment even without slip [1], [2], [3].

Directional stability deserves special interest. It has been shown that forebody of the aircraft with good characteristics at high angles of attack makes a significant positive contribution to the directional stability at high angles of attack where the vertical tail ceases to be effective. Flight data showed that at high angles of attack nose began to act unbalanced forces and moments. Experiments in the small-scale aero and hydrodynamic wind tunnels have convincingly shown that the aerodynamic phenomenon that causes asymmetrical forces and moments is the development of intense vortex system coming down from the nose part of the aircraft [4].

International practice of maneuverable aircraft engineering shows tendency of avoiding an oval cross section noses towards to more compound shapes. On the one hand, these changes are needed to meet invisibility requirements. However, further improvement of the aerodynamic performance is impossible without an essential change in the nature of the flow around forebody. One of the key change in maneuverable aircraft design is the presence of a sharp edge on the forebody, and asymmetry of the upper and lower half of nose section. Currently, all of the existing or developing aircraft of this type have a sharp edged asymmetric forebody. Vortex system arising at sharp edge does not change its origin position, so the behaviour of the vortex system is more predictable compared to the flow around the oval forebody without edge and leading edge extension on wing.

2. Wind Tunnel experiments

The aim of this work was to investigate the development of a vortex system formed over the forebody of a research model (a fuselage and a wing) at subsonic speed and high angles of attack, and the effect of a sideslip on it. For the numerical simulation a typical forebody of maneuverable aircraft was selected with a chine all along the length of the model and asymmetric upper and lower cross-sectional shapes. The length of the model under consideration was 1.6 m with the wingspan of 1.2 m. In order to study its directional stability characteristics an experiment in TsAGI T-102 low speed wind tunnel was conducted. The Mach number in the experiment was $M = 0.15$, the model was tested in the range of angle of attack α from -5 to 34 deg. The sideslip angle was ranged from -20 to 20 deg. The Reynolds number was $Re = 2.1\times10^6$. General view of the research model is presented in Figure 1.

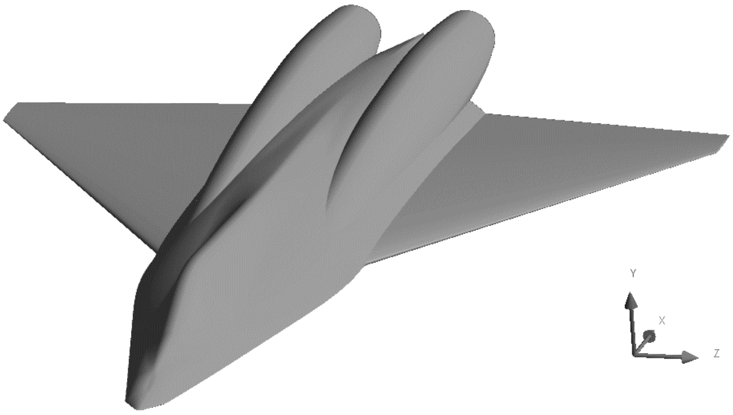

Figure 1: General view of the research model

2.1 Experimental results

The results of the experiment showed small directional instability of the model in the almost entire range of angles of attack, meanwhile at angles of attack above 30 deg. model became directionally stable (Figures 2 and 3). To investigate this phenomenon a numerical simulation was carried out.

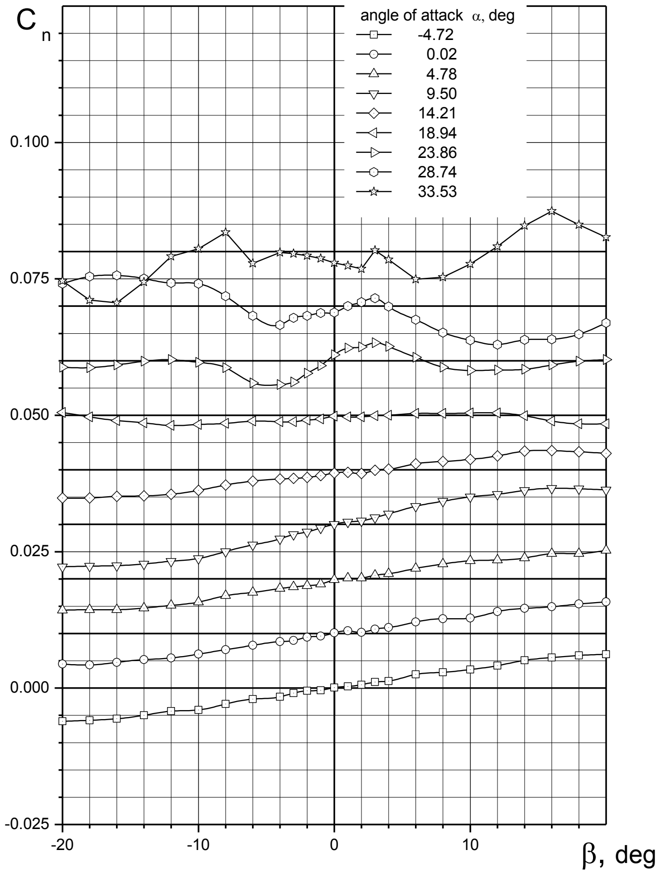

Figure 2: The yaw moment coefficient of the model at different angles of attack

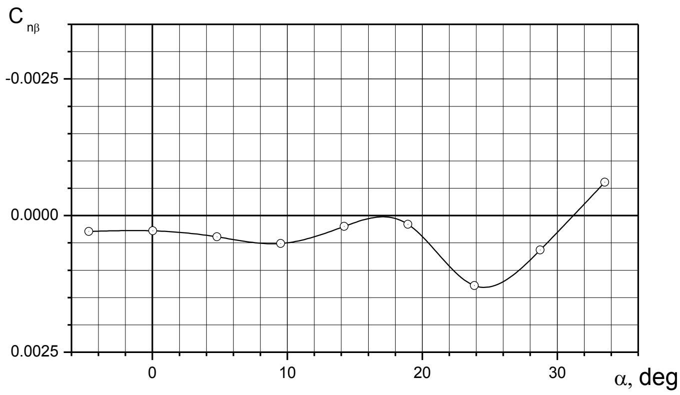

Figure 3: The derivative of the yaw moment coefficient of the model with respect to the sideslip angle versus the angle of attack

3. Computational modelling

Solution process was consisted of three stages. At first stage, mathematical model was built in a CAD/CAE program. Then, the computational mesh was created using the program ICEM CFD. In the third phase, numerical simulation of the flow around the model was performed using the ANSYS CFX software. A series of calculations has been carried out in three-dimensional formulation on a structured multi-block grid. Time-averaged Navier-Stokes equations with the k-ω SST turbulence model were solved. Second order approximation scheme was used for all equations. A rectangular parallelepiped extended 20 chords upstream, 20 chords downstream and 20 chords in each side direction was chosen as a computational domain. The total number of cells was about 25 million. Shown in Figure 4 is surface mesh on the model. The free stream velocity at front boundary was set to 50 m/s, the ambient temperature T = 288K. Excessive static pressure was set at the rear boundary to be equal to 0 Pa. At side boundaries it was set to be equal to 0 Pa as well. All relevant parameters were taken in accordance with the international standard atmosphere. Calculations were carried out at angles of attack 24, 34 deg., and sideslip angles 2, 4 and 8 deg.

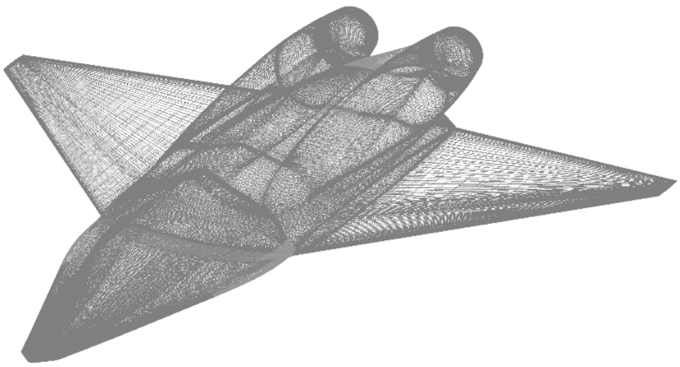

Figure 4: General view of created mesh

3.1 Computational results

The results of simulation show the presence of a system of two vortices at the apex of the forebody. At sideslip angles 2 and 4 deg. an appropriate correlation with the experimental data was obtained. Figure 5 shows a comparison of the numerical simulation with the experimental data. As can be seen the numerical results qualitatively correctly reflect the directional stability variations obtained in the experiment. To illustrate the difference in forebody vortex system at angles of attack of 24 and 34 deg a set of six cross sections of interest was chosen (Figure 6). The x-component of flow vorticity and pressure coefficient distributions at these cross sections are shown in Figures 7-18. One can see a significant difference in flowfields at angles of attack under consideration. At angle of attack of 34 deg. the strength of vortices and its position relative to the model form specific pressure distribution on the model surface, which causes a force acting opposite to sideslip, which gives rise to the model directional stability. To summarize influence of vortex system on directional stability, the pressure coefficient distribution on model’s upper surface at investigated angles of attack are presented in Figures 19-20. One can see that vortex system at 34 deg. has significantly greater intensity, which results in positive contribution to the directional stability of investigated model. Another way to illustrate the existence of side force is presented in Figures 21 and 22 where the pressure coefficient distributions at cross-section 2 and 3 were plotted. These plots show that rarefaction at the windward side of the forebody is higher than at the leeward one, which gives rise to the stabilising side force. At angle of attack of 24 deg that rarefaction difference is seen to be significantly lower than at 34 deg. so it's insufficient to provide for directional stability of the model.

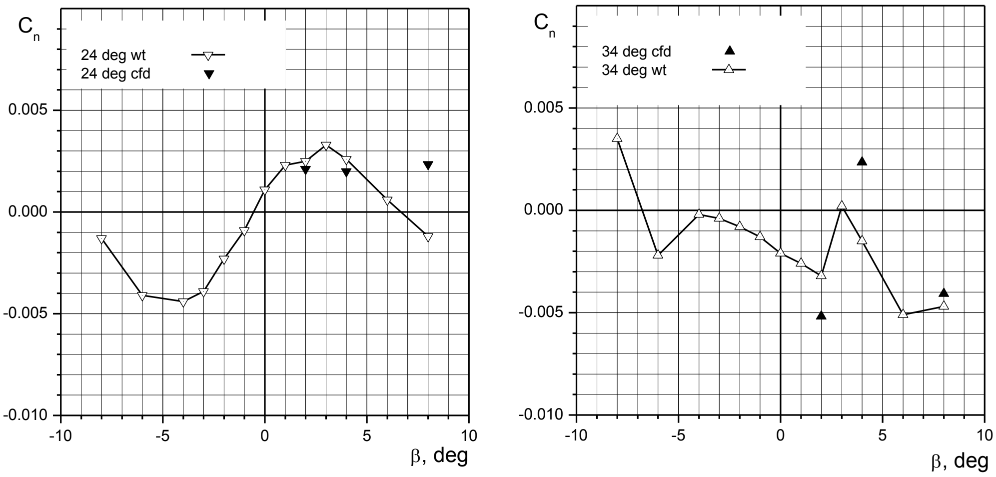

Figure 5: Comparison of experimental data and numerical simulations for yaw moment coefficient of the model at angles of attack of 24 and 34 deg.

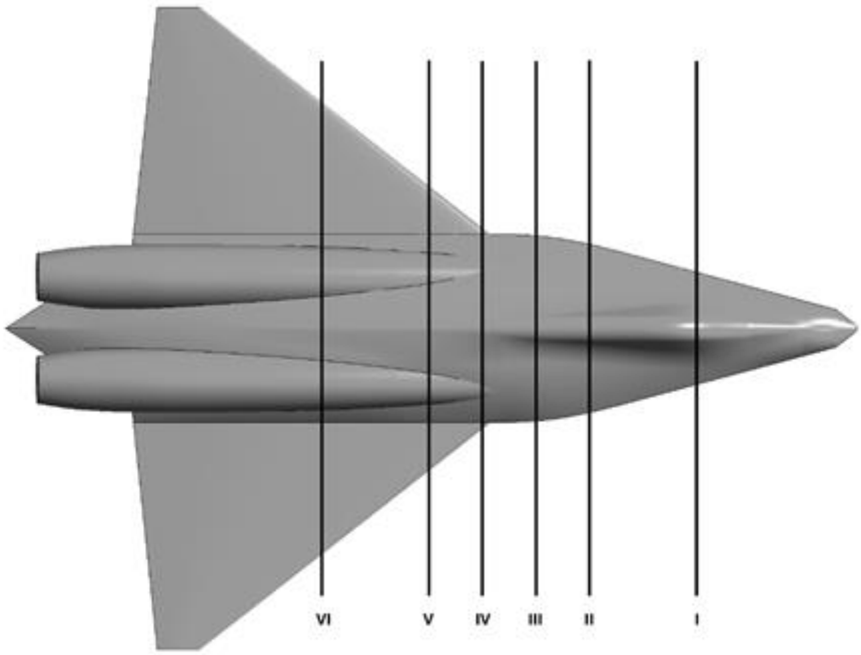

Figure 6: Cross section set considered

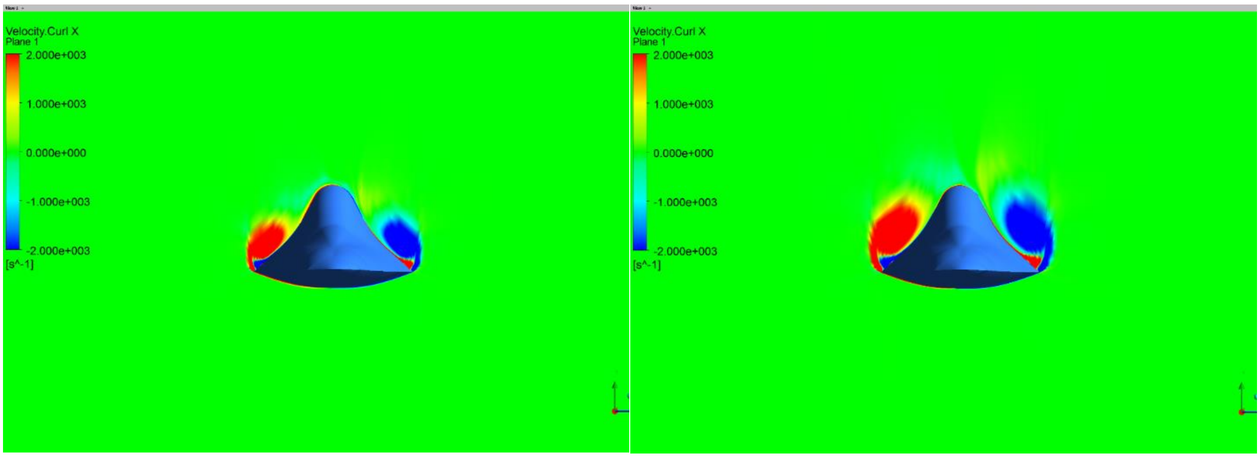

Angle of attack 24 deg. Angle of attack 34 deg.

Figure 7: X-component of the vorticity distribution in cross-sectional plane I at sideslip angle 2 deg.

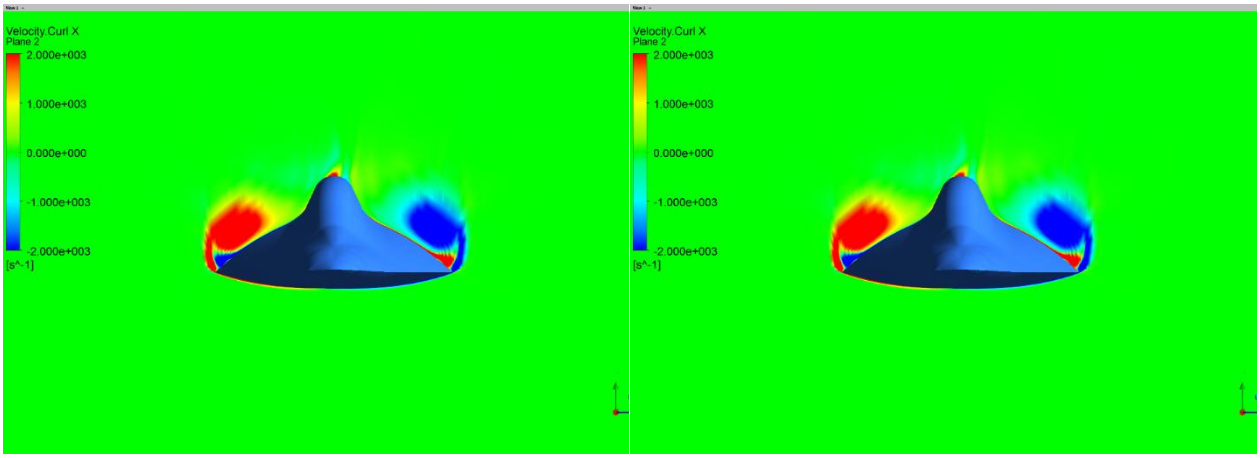

Angle of attack 24 deg. Angle of attack 34 deg.

Figure 8: X-component of the vorticity distribution in cross-sectional plane II at sideslip angle 2 deg.

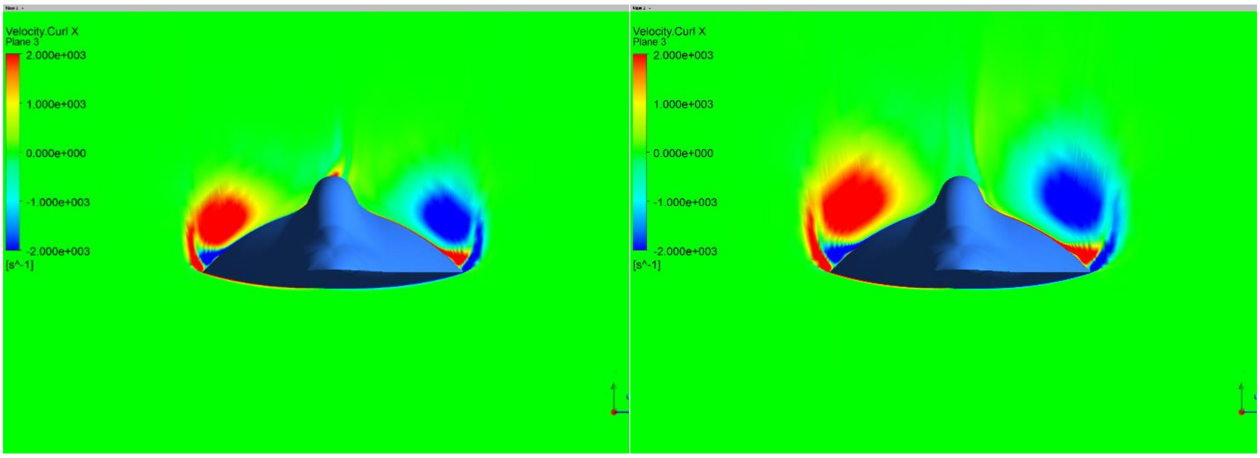

Angle of attack 24 deg. Angle of attack 34 deg.

Figure 9: X-component of the vorticity distribution in cross-sectional plane III at sideslip angle 2 deg.

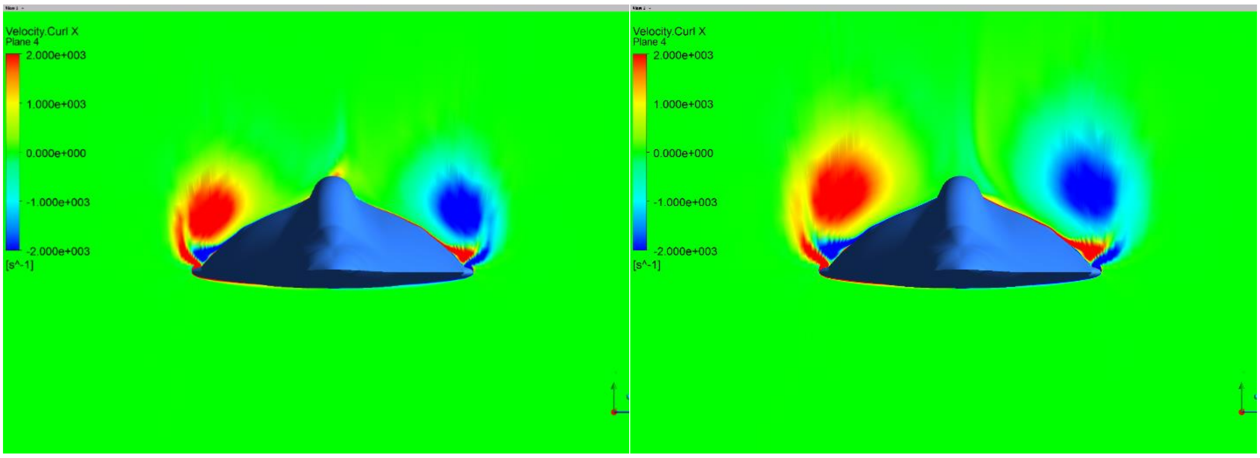

Angle of attack 24 deg. Angle of attack 34 deg.

Figure 10: X-component of the vorticity distribution in cross-sectional plane IV at sideslip angle 2 deg.

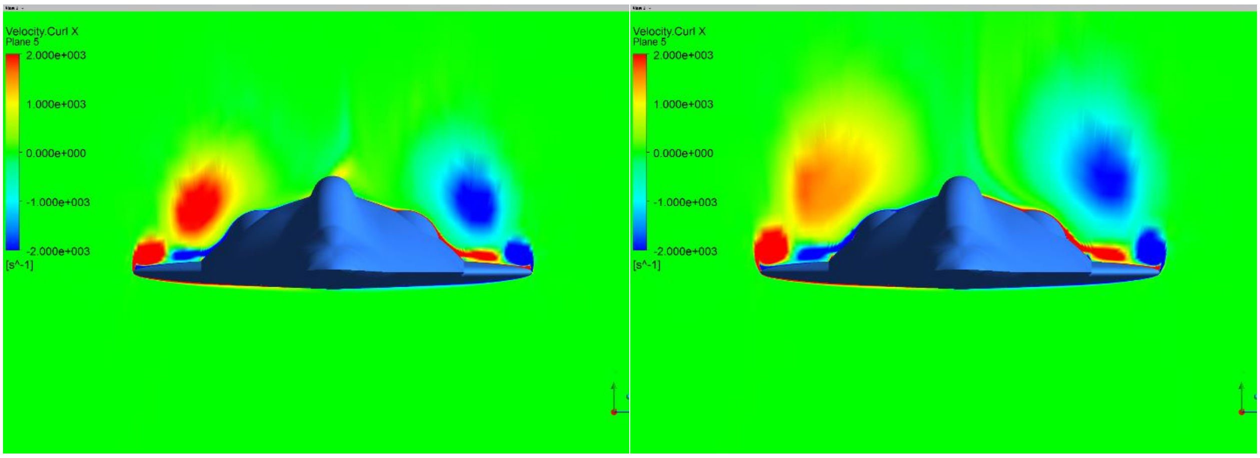

Angle of attack 24 deg. Angle of attack 34 deg.

Figure 11: X-component of the vorticity distribution in cross-sectional plane V at sideslip angle 2 deg.

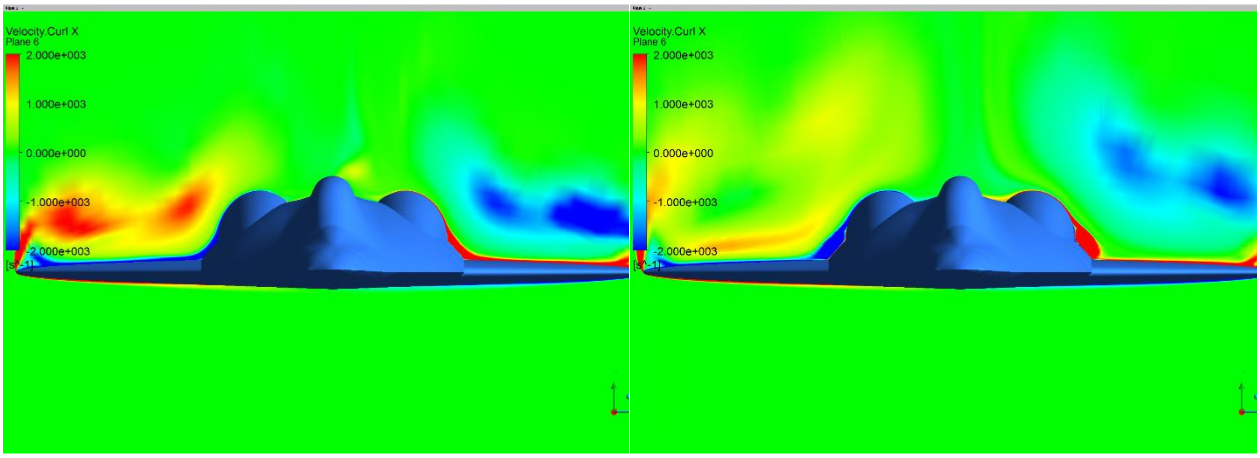

Angle of attack 24 deg. Angle of attack 34 deg.

Figure 12: X-component of the vorticity distribution in cross-sectional plane VI at sideslip angle 2 deg.

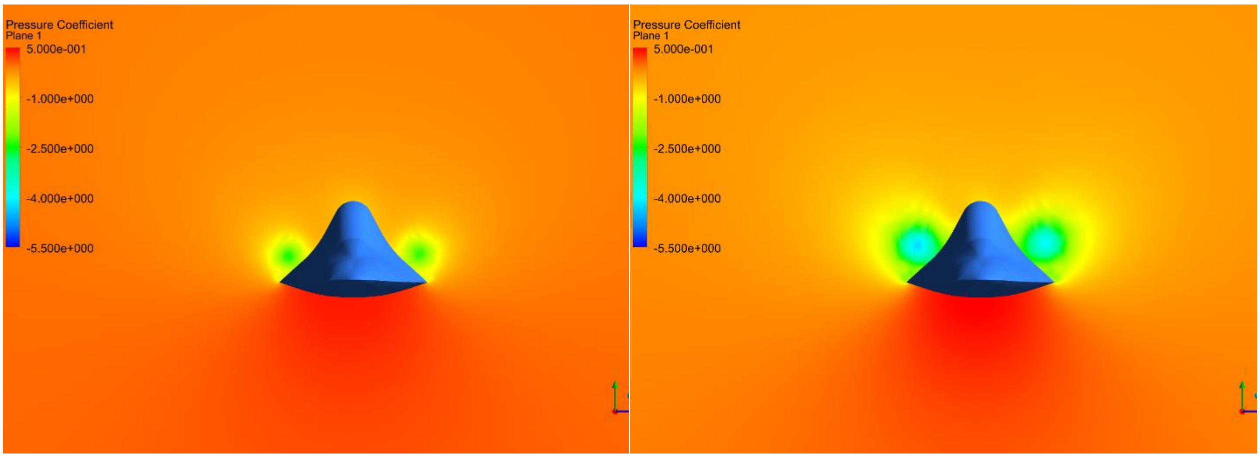

Angle of attack 24 deg. Angle of attack 34 deg.

Figure 13: Pressure coefficient distribution in cross-sectional plane I at sideslip angle 2 deg.

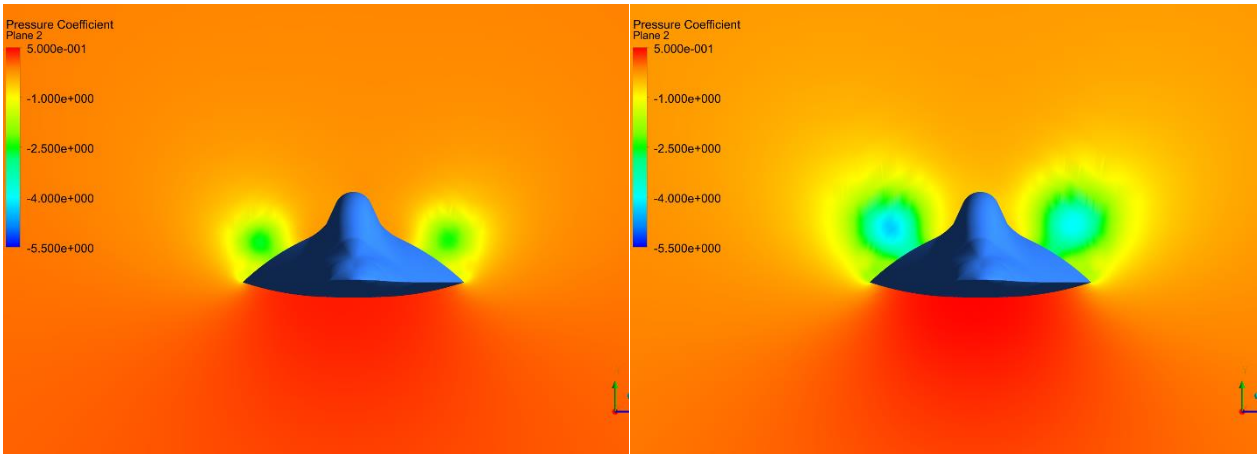

Angle of attack 24 deg. Angle of attack 34 deg.

Figure 14: Pressure coefficient distribution in cross-sectional plane II at sideslip angle 2 deg.

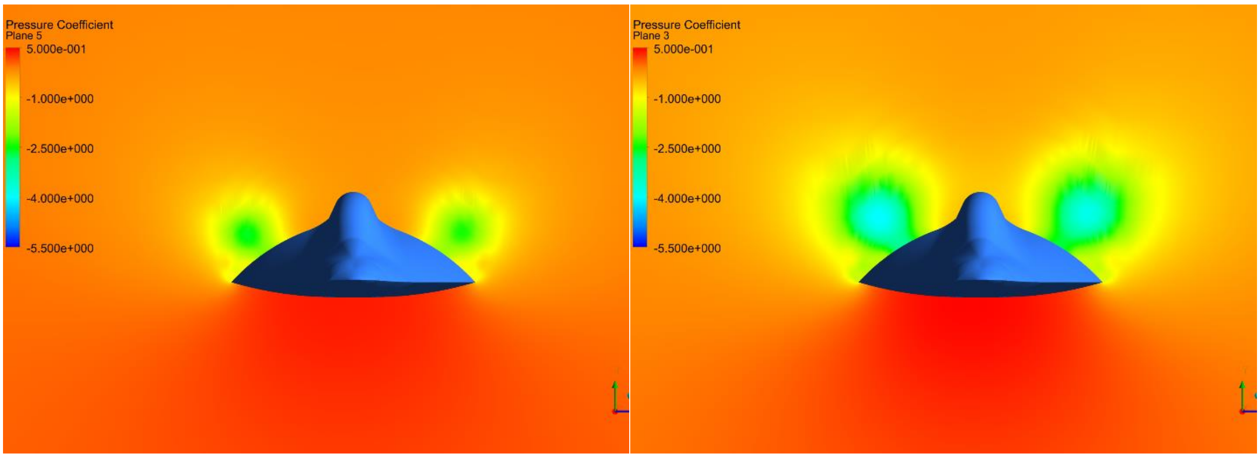

Angle of attack 24 deg. Angle of attack 34 deg.

Figure 15: Pressure coefficient distribution in cross-sectional plane III at sideslip angle 2 deg.

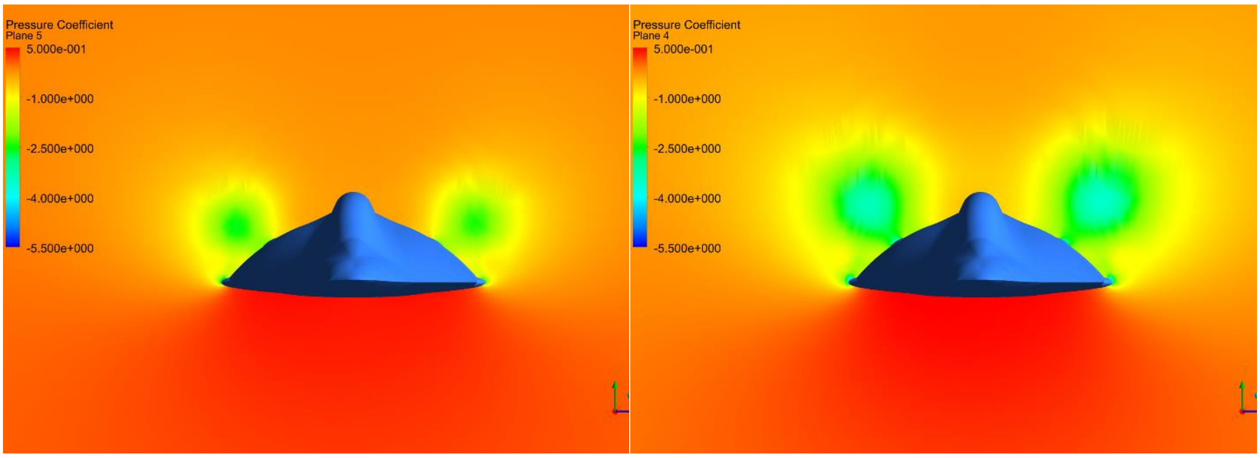

Angle of attack 24 deg. Angle of attack 34 deg.

Figure 16: Pressure coefficient distribution in cross-sectional plane IV at sideslip angle 2 deg.

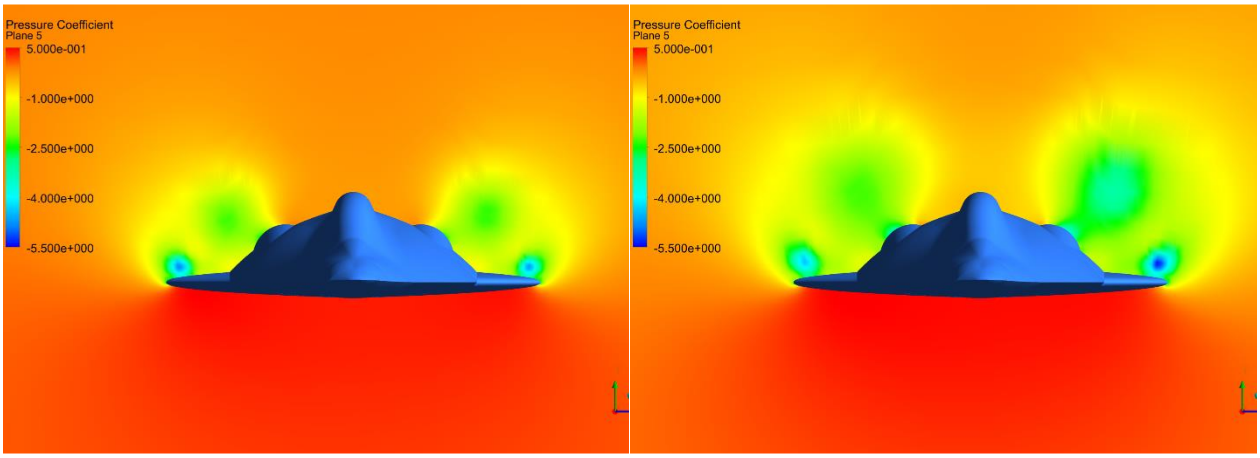

Angle of attack 24 deg. Angle of attack 34 deg.

Figure 17: Pressure coefficient distribution in cross-sectional plane V at sideslip angle 2 deg.

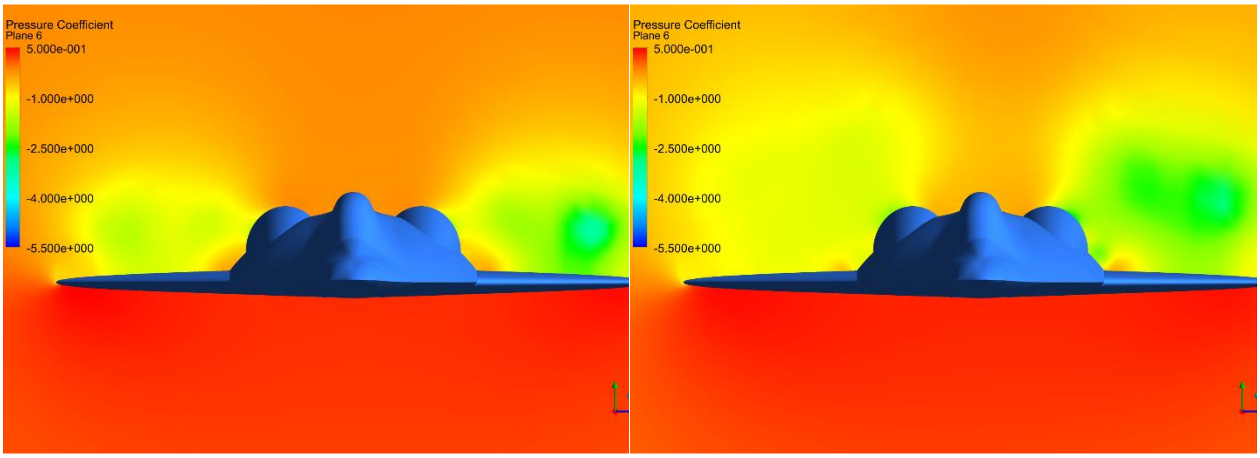

Angle of attack 24 deg. Angle of attack 34 deg.

Figure 18: Pressure coefficient distribution in cross-sectional plane VI at sideslip angle 2 deg.

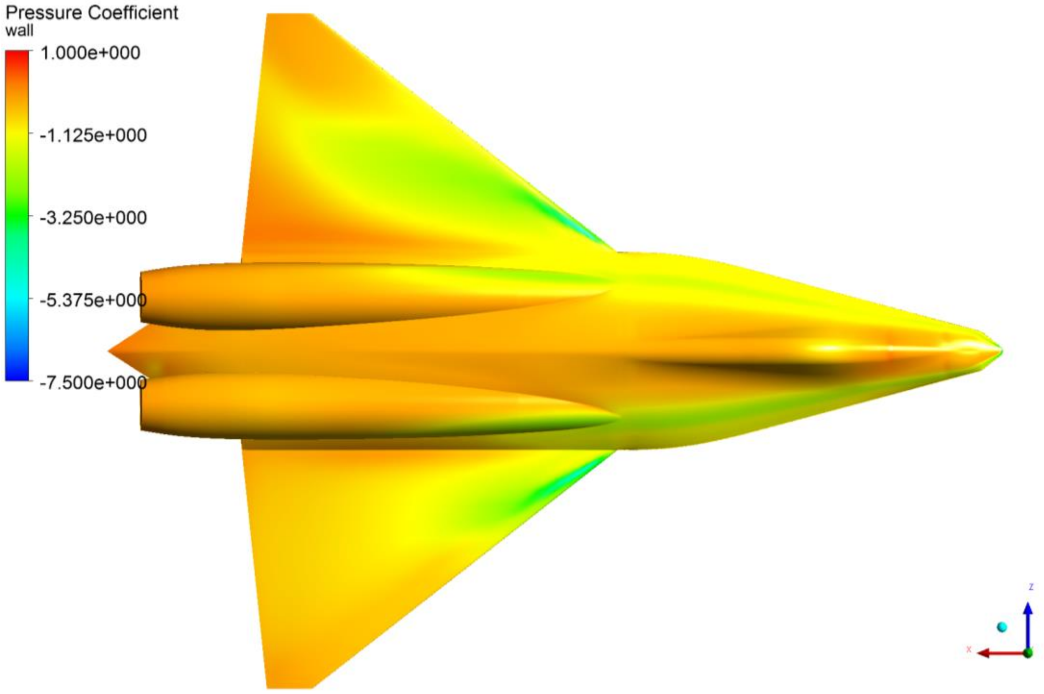

Figure 19: Pressure coefficient distribution on model’s upper surface at angle of attack of 24 deg. and sideslip angle 2 deg.

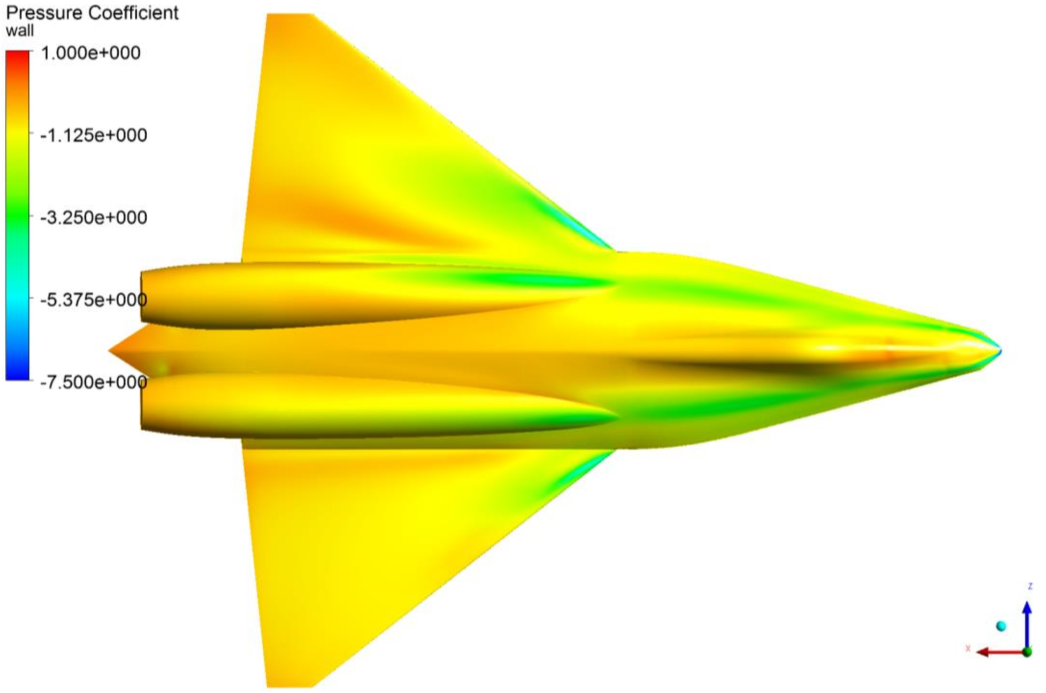

Figure 20: Pressure coefficient distribution on model’s upper surface at angle of attack of 34 deg. and sideslip angle 4 deg.

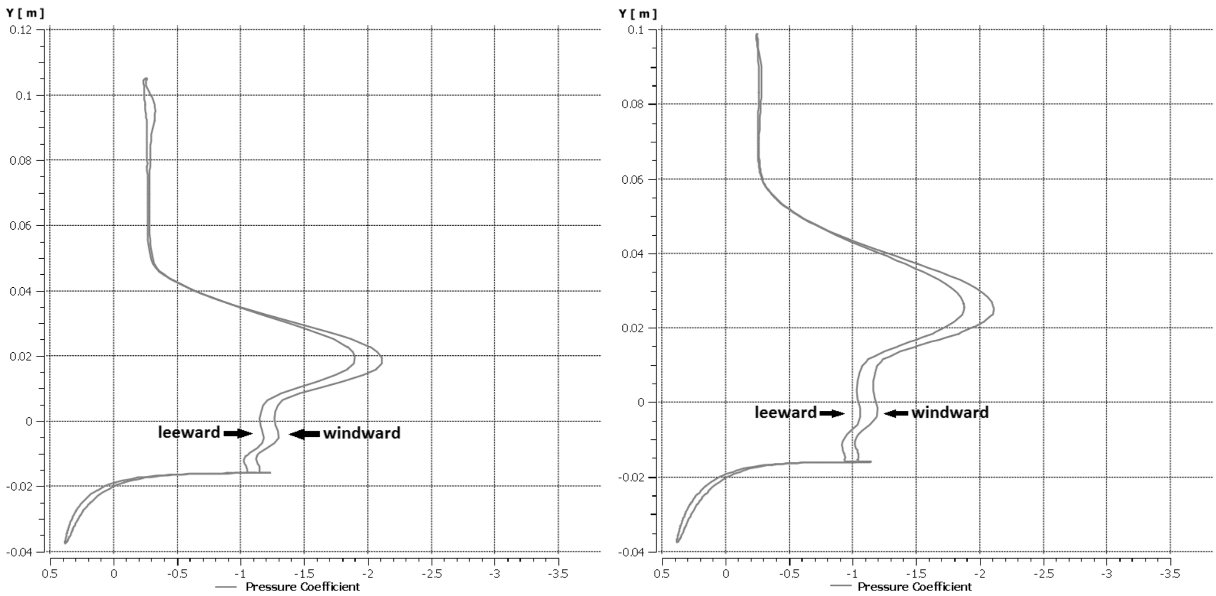

Figure 21: Pressure coefficient distribution on intersection of model and planes 2 (left) and 3 (right). Angle of attack 24 deg.

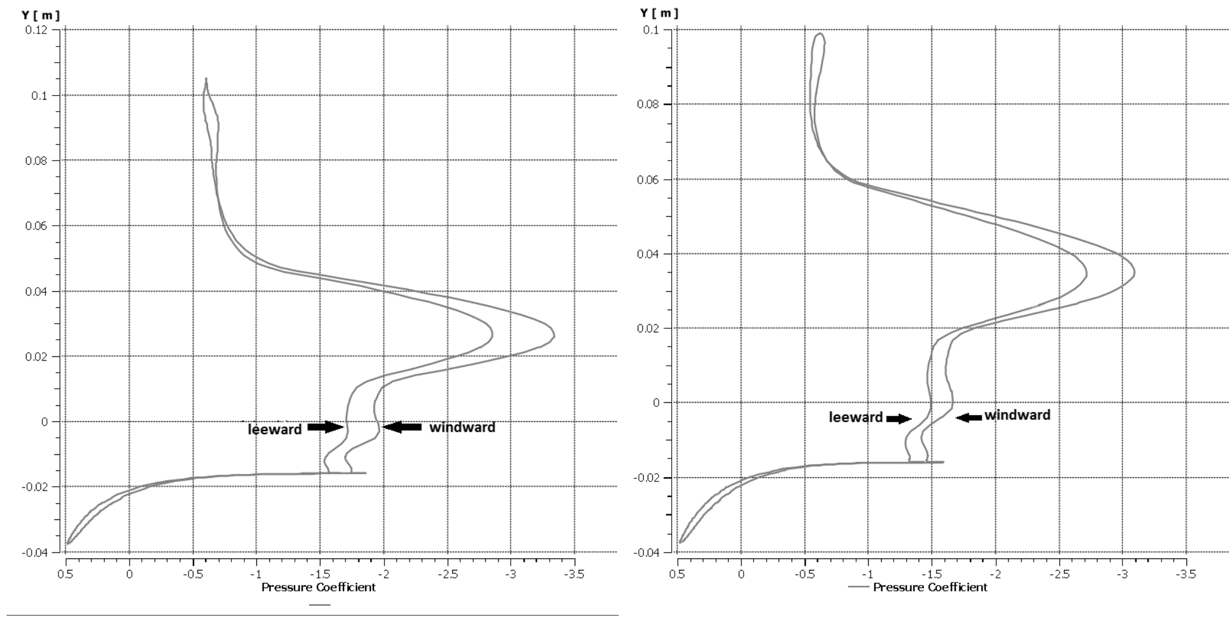

Figure 22: Pressure coefficient distribution on intersection of model and planes 2 (left) and 3 (right). Angle of attack 34 deg.

4. Conclusions

A series of RANS simulations of subsonic flow around research model of maneuverable aircraft at high angles of attack and nonzero sidesleep was carried out. It was shown that at high angle of attack a system of vortices is formed over the forebody. The asymmetry in the strength and positions of these vortices at high angles of attack and nonzero side-sleep angle results in increasing rarefication at the windward side of the forebody and decreasing it at the leeward one which in turn contributes to the directional stability of the model. The numerical results was shown to qualitatively correctly reflect the experimentally obtained variations of the yaw moment coefficient of the model with angles of attack and sidesleep. This makes foundation for applying the approach used in the current work to studying the behavior of the vortex system on aircraft forebody.

References

[1] R. Ravi and William H. Masont. 1994. Chine-Shaped Forebody Effects on Directional Stability at High-a. Virginia Polytechnic Institute and State University, *Journal of Aircraft Vol. 31, No.3, May-June 1994*.

[2] N. M. Komerath, S. G. Liou, R. J. Schwartz, and J. M. Kim. 1992. Flow over a Twin-Tailed Aircraft at Angle of Attack Part I: Spatial Characteristics. Georgia Institute of Technology, *Journal of Aircraft Vol. 29, No.3, May-June 1992*.

[3] Michael R. Mendenhall and Daniel J. Lesieutret Nielsen. 1992. Prediction of Vortex Shedding from Forebodies with Chines. Engineering & Research, Inc., *Journal of Aircraft Vol. 29, No.3, May-June 1992*.

[4] Kenneth E. Wurtzler. 2000. Computational Analysis of F-15 Forebody Flow at High Alpha, U.S. Air Force Research Laboratory, Wright-Patterson Air Force Base, *Journal of Aircraft Vol 37,No.5, September 2000*